THE JOURNAL OF PHYSICAL CHEMISTRY A

Article

pubs.acs.org/JPCA

Photo-oxidation of Dimethyl Malonate Initiated by Chlorine Atoms in Gas Phase: Kinetics and Mechanism

Guido N. Rimondino, Diana P. Henao, Walter J. Peláez, Gustavo A. Argüello, and Fabio E. Malanca*

Instituto de Investigaciones en Fisicoquímica de Córdoba (INFIQC) CONICET, Departamento de Físico Química, Facultad de Ciencias Químicas (Universidad Nacional de Córdoba), Ciudad Universitaria (X5000HUA), Córdoba, República Argentina

ABSTRACT: The rate coefficient for the gas-phase reaction of chlorine atoms with dimethyl malonate (DMM, $CH_3OC(O)CH_2C(O)OCH_3$) was determined at 298 K using relative methods giving a value of $(3.8 \pm 0.4) \times 10^{-12}$, cm^3 $molecule^{-1}$ s^{-1}). The photo-oxidation mechanism of DMM was also investigated. The main products were identified by infrared spectroscopy, and computational calculations were performed in order to support the experimental data. The results reveal that the photo-oxidation occurs mainly by the abstraction of an H atom from the methyl groups. The $CH_3OC(O)CH_2C(O)OCH_2O^{\bullet}$ radical formed subsequently reacts according to three competitive paths: reaction with molecular oxygen to yield $CH_3OC(O)CH_2C(O)OC(O)H$, isomerization−unimolecular decomposition to lead finally to $CH_3OC(O)C(O)H$, CO_2, and HC(O)OH, and α-ester rearrangement to form monomethyl malonate and carbon monoxide. The yield of products as a function of oxygen pressure was also determined.

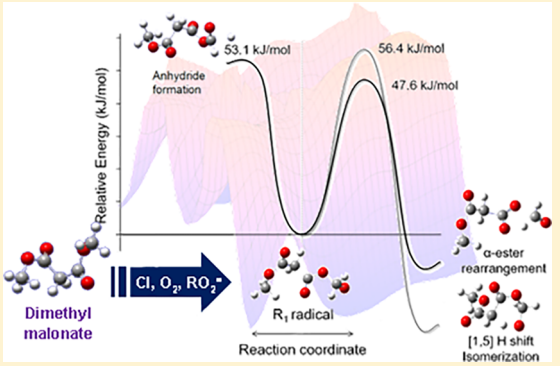

INTRODUCTION

Dibasic esters (DBEs, $ROC(O)(CH_2)_nC(O)OR$) represent a large family of organic compounds. Most popular DBEs result in derivative structures of malonic (n = 1), succinic (n = 2), glutaric (n = 3), and adipic (n = 4) acids and are used as solvents or industrial additives.[1−3] Due to their vast production and usage, this family was investigated in order to determine their impact to the atmosphere.

Kinetic studies of DBEs (dimethyl succinate, glutarate, and adipate) with $^{\bullet}OH$ radicals and chlorine atoms were carried out by Aschmann and Atkinson,[4] while their photo-oxidation mechanisms in the gas phase were reported by Cavalli et al. and Tuazon et al.[5,6]

Although the use of malonates is widespread at industrial scale, studies on degradation of malonates in gas phase are scarce. They are especially important due to their wide use in the so-called "malonic ester synthesis". This synthetic procedure is a useful methodology in which carbon−carbon bonds are formed by the nucleophilic attack of the diester enolate to an alkyl halide in a S_N2 reaction. As a result, mono- and di- alkylacetic acid derivatives are obtained by a simple methodology. In this sense, malonates were used in the synthesis of different pharmaceutical principles such as barbituric acid and its derivatives, vitamins, and artificial flavorings and fragrances.[7−10]

Rate coefficients for reaction with chlorine atoms as well as a photo-oxidation mechanism have only been reported very recently by our group for di-*tert*-butyl malonate (DTBM, $(CH_3)_3COC(O)CH_2C(O)OC(CH_3)_3$), where k was calculated as $(1.5 \pm 0.1) \times 10^{-10}$ cm^3 $molec^{-1}$ s^{-1}.[11]

In order to determine the impact of dimethyl malonate (DMM, $CH_3OC(O)CH_2C(O)OCH_3$) emissions to the atmosphere, the present study extends the knowledge to the determination of the rate coefficient with chlorine atoms (used as surrogate of OH radicals) and its photo-oxidation mechanism, both supported by experimental measurements and computational studies.

Values of rate coefficients for the reaction of chlorine atoms with the corresponding longer chain molecules, such as dimethyl succinate ($CH_3OC(O)CH_2CH_2C(O)OCH_3$, DMS), glutarate ($CH_3OC(O)CH_2CH_2CH_2C(O)OCH_3$, DMG), and adipate ($CH_3OC(O)CH_2CH_2CH_2CH_2C(O)OCH_3$, DMA) were reported as (0.68 ± 0.09), (1.9 ± 0.3), and $(6.1 \pm 0.9) \times 10^{-11}$ cm^3 $molec^{-1}$ s^{-1}, respectively.[4] Those values suggest that the reactivity of DMM should be lower and consequently its atmospheric lifetime longer.

EXPERIMENTAL SECTION

Chemicals. The following chemicals were used as purchased: DMM (98%, ICN Biomedicals Inc.), acetone (Sintorgan), methyl formate (98%, Sigma-Aldrich), and formic acid (90%, Dorwil). Commercially available oxygen (4.8; AGA), nitrogen (4.8; AGA), and carbon monoxide (2.0; Praxair) were used as received. Chlorine (>98% purity) was synthesized by direct reaction between HCl and $KMnO_4$ in a nitrogen flux, collected at liquid N_2 temperatures, and further distilled.

Methods. Experimental determinations were carried out in a conventional glass vacuum line equipped with two

Received: July 5, 2017
Revised: October 24, 2017
Published: October 25, 2017

DOI: 10.1021/acs.jpca.7b06595
J. Phys. Chem. A XXXX, XXX, XXX−XXX

capacitance pressure gauges (0−1000 mbar, MKS Baratron; 0−70 mbar, Bell and Howell). A photoreactor consisting of a 5 L glass bulb surrounded by black lamps was used to photolyze the mixtures of reactants. The progress of reactions was followed using a Fourier transform infrared spectrometer (Bruker IFS-28) and a long path (9.0 m) infrared gas cell. Spectra were recorded with a resolution of 2 cm^{-1}.

For the photolysis experiments, 5 to 7 μL of DMM were injected to the previously evacuated photoreactor through a silicone/PTFE septum. This procedure was undertaken due to the relatively low vapor pressure of DMM at room temperature and was followed by addition of chlorine (0.35 mbar) and either N_2 (for determination of the rate coefficients) or O_2 (for photo-oxidation experiments) to reach atmospheric pressure. Control experiments were performed in the darkness to check for the presence of heterogeneous or dark reactions.

Kinetic experiments of DMM with chlorine atoms were carried out using a relative method. This is a reliable technique for measuring rate coefficients using as reference a compound whose rate coefficient is known and presents no complications such as unwanted secondary reactions.[12] For these reasons, acetone and methyl formate were used as references, and the experimental data obtained were plotted to conform with eq 1, from which the rate coefficient of the reactant is inferred.

$$\ln\left(\frac{[\mathrm{DMM}]_0}{[\mathrm{DMM}]_t}\right) - k_{\mathrm{wall}} \times t = \frac{k_{\mathrm{DMM}}}{k_{\mathrm{reference}}} \ln\left(\frac{[\mathrm{reference}]_0}{[\mathrm{reference}]_t}\right) \quad (1)$$

Here, $[DMM]_0$, $[DMM]_t$, $[reference]_0$, and $[reference]_t$ indicate DMM and reference concentrations at the beginning and after the irradiation time, respectively. The rate coefficients k_{DMM} and $k_{reference}$ correspond to the reactions of chlorine atoms with DMM and reference, respectively. The plot of $\ln([DMM]_0/[DMM]_t)$ vs $\ln([reference]_0/[reference]_t)$ should be linear, and the slope should correspond to the ratio $k_{DMM}/k_{reference}$. The value of k_{wall} (which accounts for overall nonphotolytic processes) in typical experiments was 9×10^{-5} s^{-1}.

Computational Details. All calculations were carried out using the Gaussian09 computational package.[13] The software was used to compare the energy requirements of relevant reaction paths of the photo-oxidation mechanism. The geometric parameters for reactants, transition states, and products were fully optimized using density functional theory with the B3LYP functional and the 6-311+G(d,p) basis set.[14]

RESULTS AND DISCUSSION

The kinetics of reaction between DMM and chlorine atoms (reaction R1) was undertaken relative to the reaction of acetone as well as methyl formate with chlorine atoms (reactions R2 and R3, respectively):

$$CH_3OC(O)CH_2C(O)OCH_3 + Cl^{\bullet} \rightarrow \text{products} \quad (R1)$$

$$CH_3C(O)CH_3 + Cl^{\bullet} \rightarrow \text{products} \quad (R2)$$

$$CH_3OC(O)H + Cl^{\bullet} \rightarrow \text{products} \quad (R3)$$

Figure 1 shows the disappearance of DMM relative to the disappearance of acetone and methyl formate according to reaction R1. From the plot, both slopes, $k_{DMM}/k_{acetone} = (1.78 \pm 0.04)$ and $k_{DMM}/k_{methyl\ formate} = (2.73 \pm 0.06)$ were obtained.

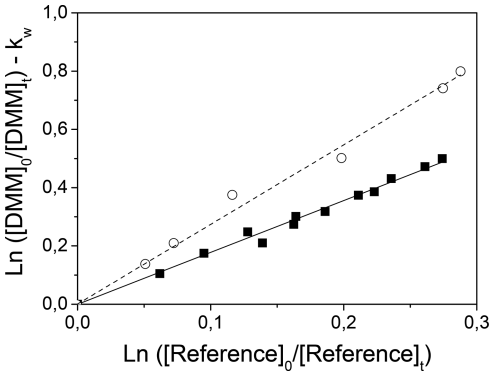

Figure 1. Kinetic data (total pressure 1000 mbar at 298 K) for the reaction of DMM with chlorine atoms relative to acetone (solid squares) and methyl formate (open circles).

Errors presented correspond to one standard deviation from the linear fit of the experimental data.

Literature values for the rate coefficient for acetone at 298 K range from 2.0 to 3.1 × 10^{-12} cm^3 $molec^{-1}$ s^{-1}.[15−23] Nevertheless, the majority of these values are comprised between 2.0 and 2.3 × 10^{-12} cm^3 $molec^{-1}$ s^{-1}, and the value recommended by IUPAC is 2.10 × 10^{-12} cm^3 $molec^{-1}$ s^{-1}.[24] Using this, $k_{DMM} = (3.7 \pm 0.5) \times 10^{-12}$ cm^3 $molec^{-1}$ s^{-1} was obtained. Similarly, the rate constants measured for methyl formate at 298 K range from 1.17 to 1.83 cm^3 $molec^{-1}$ s^{-1},[25] and considering a mean value of 1.4 × 10^{-12} cm^3 $molec^{-1}$ s^{-1} also used by Good et al.,[26] $k_{DMM} = (3.8 \pm 0.3) \times 10^{-12}$ cm^3 $molec^{-1}$ s^{-1} was obtained. The error associated in both cases was assumed as the mean value of the interval between the lowest and highest values reported for $k_{acetone}$ and $k_{methyl\ formate}$, respectively, because the standard deviation of our data would give lower numbers. As can be seen, both k_{DMM} values are close to each other. Thus, our recommended value is $(3.8 \pm 0.4) \times 10^{-12}$ cm^3 $molec^{-1}$ s^{-1}.

Our rate coefficient fits well within the trend previously reported for dibasic esters, $CH_3OC(O)(CH_2)_nC(O)OCH_3$ (n = 2−4), by Cavalli et al. (who made a correlation between the rate constants and the number of methylene groups), with values of $(6.8 \pm 0.9) \times 10^{-12}$ for DMS (n = 2); $(19 \pm 3) \times 10^{-12}$ for DMG (n = 3); and $(61 \pm 9) \times 10^{-12}$ for DMA (n = 4).[5] In this sense, our value of $(3.75 \pm 0.4) \times 10^{-12}$ cm^3 $molec^{-1}$ s^{-1} locates itself at the lower end of the trend as expected for a moiety having only one methylene group.

A good way of giving confidence to an experimental result relies on the structure−activity relationship (SAR) method developed by Atkinson.[27,28] It allows the calculation of the rate coefficient based on the estimation of $-CH_3$, $-CH_2-$, and >CH− group rate constants (k_{prim}, k_{sec}, and k_{tert}, respectively) and the parameter factors (F) for the substituents bonded to these groups in the molecule. The reported values for the rate constant used in the calculation were $k_{prim} = 3.32 \times 10^{-11}$, $k_{sec} = 8.34 \times 10^{-11}$ (both in units of cm^3 $molec^{-1}$ s^{-1}), while the substituent factors were $F(-CH_3) = 1.00$, $F(-CH_2-) = 0.79$, $F(-CO) = 0.04$, and $F(C(O)O-) = 0.05$.[25] The estimation of the rate coefficient finally led to a value of 3.45 × 10^{-12} cm^3 $molec^{-1}$ s^{-1}, which is in excellent agreement with the present experimental value. The use of these substituent factors, and $F(-CH_2C(O)O) = 0.46$, needed to estimate the rate coefficient for dibasic esters leads to 6.4 for DMS; 19 for DMG; and 69 for DMA (in unit of 10^{-12} cm^3 $molec^{-1}$ s^{-1}).

DOI: 10.1021/acs.jpca.7b06595
J. Phys. Chem. A XXXX, XXX, XXX−XXX

These values corroborate the reliability of the SAR method for this kind of compounds.

Additionally, the SAR reactivity for methyl and methylene groups gives a percentage of 96 and 4, thus suggesting that reactivity of the methylene group in DMM is of minor importance and that the main degradation path should involve methyl groups.

Photo-oxidation Products. Figure 2 shows the infrared spectra obtained in the photo-oxidation initiated by chlorine atoms at 298 K and at an oxygen pressure of 760 Torr. First and second traces correspond to the spectra obtained after and before 40 min of irradiation. Subsequent subtraction of the second from the first trace (appropriately scaled) leads to the third trace corresponding to products in which the appearance of carbon monoxide and carbon dioxide (bracketted bands) is evident.

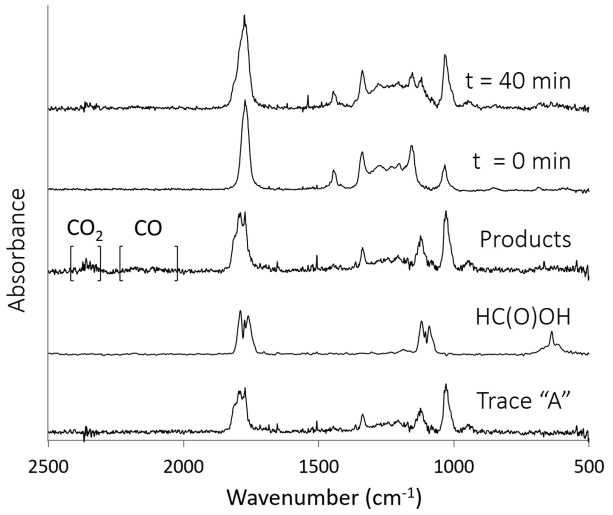

Figure 2. Infrared spectra obtained in the photo-oxidation of DMM. Traces from top to bottom: after 40 min of irradiation, before irradiation, products, and formic acid reference spectrum. Trace "A" is the result of subtraction of CO_2, CO, and HC(O)OH from the "Products" trace.

An analysis of the "Products" trace shows the typical signal at 637 cm^{-1}, corresponding to HC(O)OH (which is presented in pure form in the fourth trace). The subtraction of CO, CO_2, and HC(O)OH from the "Products" spectrum, leads to trace "A", where several bands can be clearly seen. In fact, the appearance of signals at around 1810 and 1030 cm^{-1} was assigned to the asymmetric C═O stretching and the C−O stretching of an anhydride group, respectively.

In an attempt to check both the stability of the products formed in our system and the possibility of looking further into the mechanism, the following experiment was set up. Samples obtained after 40 min of photolysis were maintained for 24 h in darkness inside the cell. Figure 3 shows the result of one experiment carried out at 760 Torr of added oxygen.

The first trace, coincident with the third trace in Figure 2, serves as the initial state of this new experiment. The second shows the spectrum after keeping the gas mixture in darkness for 24 h. Their comparison reveals the complete disappearance of the anhydride signals (down pointing arrows) and the increase of formic acid (up pointing arrows).

The subtraction of CO, CO_2, and HC(O)OH from the second trace gives the spectrum corresponding to residuals,

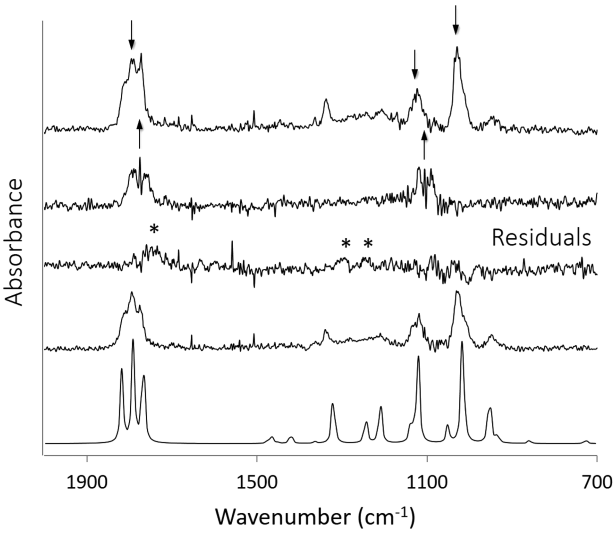

Figure 3. Spectroscopic analysis of products. From top to bottom: products after 40 min of photolysis, products formed after 24 h in darkness, and residuals resulting from the subtraction of formic acid from the second trace. Fourth and fifth traces show the experimental and calculated spectra of $CH_3OC(O)CH_2C(O)OC(O)H$, respectively.

which shows weak and not-well resolved signals (marked with asterisks) at around 1747, 1293, and 1235 cm^{-1}, which could be methyl glyoxylate, based on our proposed mechanism.

The fourth trace was obtained by the subtraction of CO, CO_2, HC(O)OH and residuals from the first trace. This spectrum presents the typical signals corresponding to an anhydride. Based on the mechanism proposed (see below), the structure of this is believed to be $CH_3OC(O)CH_2C(O)OC(O)H$.

In order to corroborate the proposed structure, the calculation of its infrared spectrum (last trace) was obtained using density functional theory with the B3LYP/6-311+G(d,p) basis set and Gaussian09 program. All frequencies were corrected with eq R1 to account for the anharmonicity of the molecule.[29]

$$\nu_{exp}/\nu_{calc} = 1.0 - 0.00001356\nu_{calc} \quad (2)$$

where ν_{exp} and ν_{calc} are the experimental and calculated wavenumbers (cm^{-1}), respectively. The new positions of the bands (1818(*sh*), 1791, 1765, 1322, 1208, 1119, 1018, and 949 cm^{-1}) are in excellent agreement (both in relative intensity as well as in peak position) with those of the experimental trace (1818, 1794, 1776, 1322, 1210, 1119, 1027, and 919 cm^{-1}). Quantification of $CH_3OC(O)CH_2C(O)OC(O)H$ was performed assuming that all the formic acid formed during the dark period comes from the decomposition of the anhydride.

Reaction Mechanism and Quantification of Photo-oxidation Products. According to the experimental results, the photo-oxidation mechanism of DMM was postulated as follows and is presented in Scheme 1.

After the attack of the chlorine atoms to any one of the six hydrogen atoms of the methyl ester groups or to one of the two hydrogen atoms of the methylene group (via "a" and "b" respectively), carbon-centered radicals are formed. They both react first with O_2 to form the corresponding peroxy radicals $(ROO)^{\bullet}$, which subsequently could react either with chlorine atoms or other peroxy radicals $(ROO)^{\bullet}$, leading to the

DOI: 10.1021/acs.jpca.7b06595
J. Phys. Chem. A XXXX, XXX, XXX−XXX

Scheme 1. Photo-oxidation Mechanism of DMM[a]

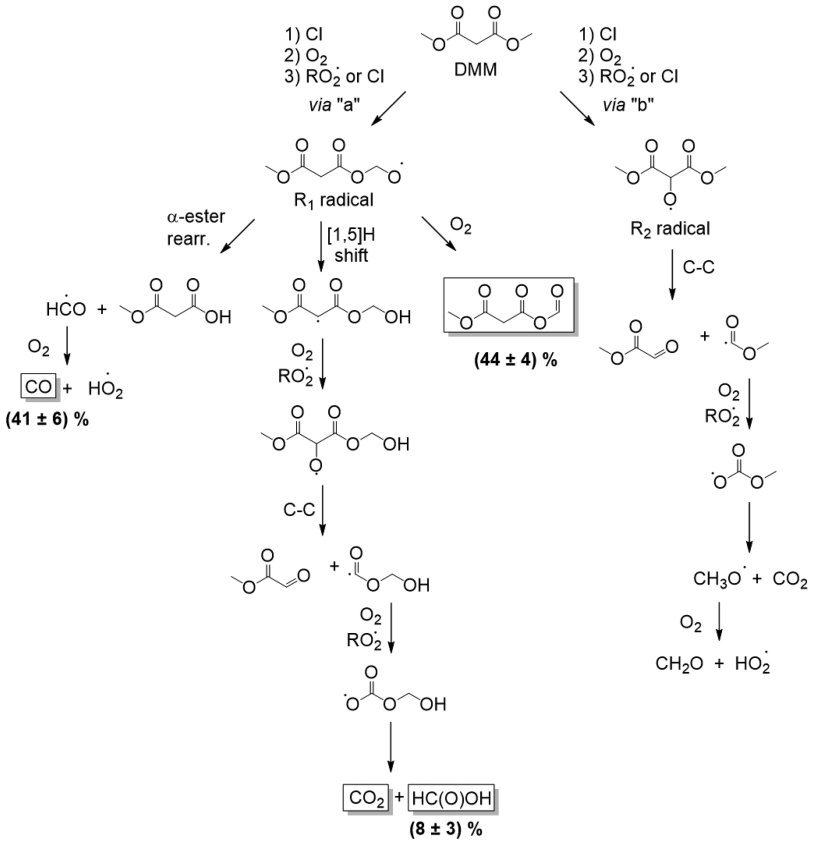

[a]Products identified are enclosed in square boxes, and percentages of formation at 760 Torr of O_2 are in bold.

formation of oxy radicals (R_1 = $CH_3OC(O)CH_2C(O)OCH_2O^•$ or R_2 = $CH_3OC(O)CHO^•C(O)OCH_3$ via "a" or "b", respectively).

In general for oxy radicals, several paths are available (fragmentation, reaction with molecular oxygen, isomerization by a hydrogen shifting, and α-ester rearrangement).[20] To the best of our knowledge, radicals with chemical structures similar to R_1 react mainly with O_2 and by α-ester rearrangement.[20,30,31] In our case, the formation of (44 ± 4)% $CH_3OC(O)CH_2C(O)OC(O)H$ (through reaction with molecular oxygen); (41 ± 6)% CO (end product from α-ester rearrangement), and (8 ± 3)% formic acid (through isomerization by H-[1,5] shifting and subsequent reactions) confirm that all these processes compete for R_1 radical. This result agrees with that obtained by Cavalli et al. for $CH_3OC(O)CH_2CH_2C(O)OCH_2O^•$, which differs from our radical only by a methylene group. Their results were (34 ± 7)% for reaction with molecular oxygen and (40 ± 10)% for α-ester rearrangement.[5]

Monomethyl malonate ($CH_3OC(O)CH_2C(O)OH$), one of the proposed products of the α-ester rearrangement, was not observed, presumably due to its very low vapor pressure. Nevertheless, the α-ester rearrangement is corroborated by the formation of CO by the very well-known reaction of $HCO^•$, as shown by reaction R4.[32]

$$HCO^• + O_2 \rightarrow CO + HO_2^• \quad \text{(R4)}$$

The assumption (cf. Figure 3) of the formation of methyl glyoxylate ($CH_3OC(O)C(O)H$) is based on the observation of formic acid as a product.

However, the abstraction of one H atom of the methylene group (via "b") leads to the formation of R_2. At this point, the rupture of the C−C bond becomes feasible, giving methyl glyoxylate and $CH_3OC(O)^•$ radical. Recall that SAR results predict a maximum of 4% for this path. If formed, $CH_3OC(O)^•$ would finally lead to CO_2 and formaldehyde. However, formaldehyde was not observed. The argument that formaldehyde is not seen because it reacts faster with Cl atoms was discarded since, if formed, observable quantities of glyoxylate and CO_2 should be present in contrast with our experimental evidence that shows glyoxylate only as a residual.

The products yield was determined as a function of the oxygen partial pressure, and the results are presented in Figure 4. Quantification of carbon monoxide and formic acid were carried out using calibration curves, performed at similar conditions as those used in our experimental system. Error bars comprise all the experimental uncertainties associated with subtraction factors and the calibration curve.

As mentioned before, the formic acid formed after 24 h of darkness was used to quantify the amount of anhydride. This procedure provides a quantitative way of assessing the importance of the reaction between R_1 and molecular oxygen, while the amounts of CO and formic acid formed during the light irradiation periods lead to the quantification of α-ester rearrangement and isomerization paths of $CH_3OC(O)CH_2(O)OCH_2O^•$ radical, respectively.

At a glance, the amount of $CH_3OC(O)CH_2C(O)OC(O)H$ increases with oxygen concentration as expected because the rate of the reaction (R_1 + O_2) increases. The depletion of R_1 concentration with increasing O_2 pressures affects considerably

DOI: 10.1021/acs.jpca.7b06595
J. Phys. Chem. A XXXX, XXX, XXX−XXX

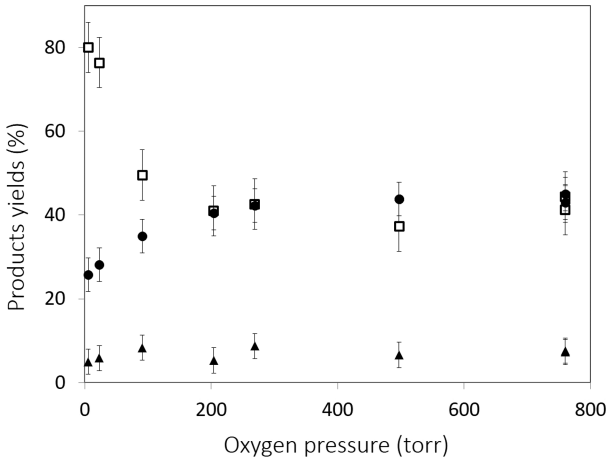

Figure 4. Yield of products as a function of molecular oxygen pressure (5−760 Torr): carbon monoxide (open squares), anhydride (solid circles), and formic acid (triangle).

the amount of R_1 available to either rearrange or isomerize, and thus, the formation of CO decreases as is clearly observed in Figure 4. A similar behavior should be expected for formic acid, though its variation is considerably smaller and difficult to appreciate because it is embedded within the error bars.

Numerical Calculations. In order to compare the energy requirements of the processes to which the oxy radicals give rise, Gaussian09 was employed to perform all the calculations. Full geometry optimizations for all the reactants, transition states, and products, were carried out, followed by analytical calculation of frequencies to determine the nature of the stationary points, that is, each structure was characterized as a minimum or a first-order saddle point by analytical frequency calculations. Intrinsic reaction coordinate calculations were performed in all cases to verify that the localized transition state structures connect with the corresponding minima stationary points associated with reactants and products.

Figure 5 shows the relative energies for the different degradation paths of R_1 radical. The energies involved for the α-ester rearrangement, the formation of $CH_3OC(O)CH_2C(O)OC(O)H$ by reaction with O_2, and the isomerization by the H-[1,5] shifting were calculated as 47.6, 53.1, and 56.4 kJ/mol, respectively.

The differences between the energy values obtained allow us to conclude that the three pathways are energetically possible, as experimentally proven. However, calculation shows that α-ester rearrangement is the most favorable path, which is corroborated looking at Figure 4 for all points below 200 Torr. At higher oxygen pressures, oxygen itself drives the kinetics because anhydride formation, which is unfavorable in terms of energy, increases its rate. However, calculations show that the isomerization is the most unfavorable path, in accordance with the quantities of formic acid observed.

CONCLUSIONS

In this work we describe the atmospheric photo-oxidation of DMM initiated by chlorine atoms. Its rate coefficient was measured, $(3.75 \pm 0.4) \times 10^{-12}$ cm^3 $molec^{-1}$ s^{-1}, and degradation products were identified and quantified. Also, degradation products were identified, and a reaction mechanism was proposed based on both, experimental and computational calculations. We also conclude that chlorine atoms attack mainly the methyl ester groups, and the oxy-radical formed at this point ($CH_3OC(O)CH_2C(O)OCH_2O^{\bullet}$) further reacts mostly via α-ester rearrangement or reaction with O_2, when it is added at high partial pressures, while isomerization by the H[1,5] shifting is a path of minor importance.

AUTHOR INFORMATION

Corresponding Author

*E-mail: fmalanca@fcq.unc.edu.ar.

ORCID

Fabio E. Malanca: 0000-0001-9289-5689

Notes

The authors declare no competing financial interest.

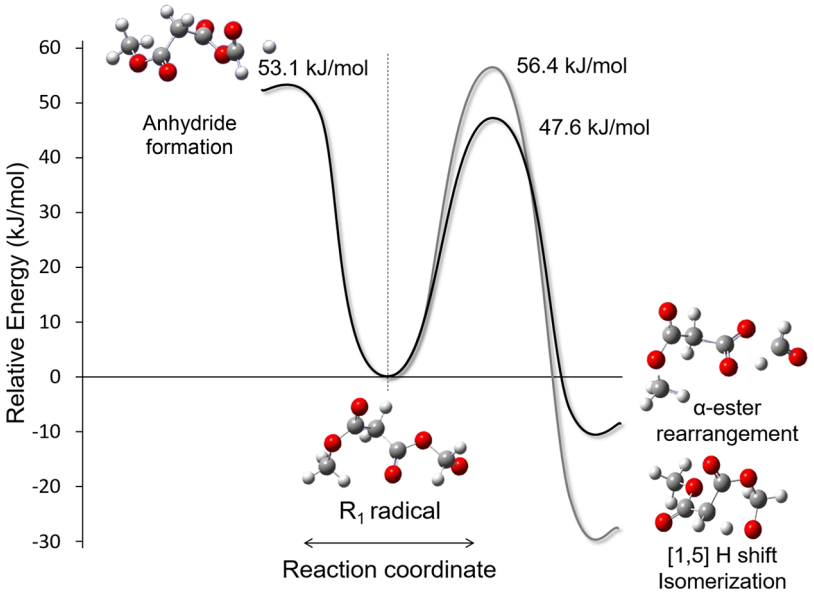

Figure 5. Reaction coordinates of R_1 radical. Top shows the formation of $CH_3OC(O)CH_2C(O)OC(O)H$ anhydride via H-abstraction, while bottom shows α-ester rearrangement and isomerization.

DOI: 10.1021/acs.jpca.7b06595
J. Phys. Chem. A XXXX, XXX, XXX−XXX

■ ACKNOWLEDGMENTS

Financial support from CONICET, ANPCyT, and SECyT-UNC is gratefully acknowledged. D.H. thanks CONICET for her Ph.D. fellowship. This work used computational resources from CCAD−Universidad Nacional de Córdoba (http://ccad.unc.edu.ar/), in particular the Mendieta Cluster, which is part of SNCAD−MinCyT, República Argentina. We also thank Dr. Lucas O. Agazzi for providing us with some reagents for complementary experiments.

■ REFERENCES

(1) Anastas, P. T.; Abraham, M. A.; Moens, L. Green Chemistry as Applied to Solvents. *Clean Solvents. Alternative Media for Chemical Reactions and Processing* **2002**, *819*, 1−9.

(2) Kob, N. E.; Abraham, M. A.; Moens, L. Dibasic Ester: A Low Risk, Green Organic Solvent Alternative. *Clean Solvents. Alternative Media for Chemical Reactions and Processing* **2002**, *819*, 238−253.

(3) Gryglewicz, S.; Stankiewicz, M.; Oko, F. A.; Surawska, I. Esters of Dicarboxylic Acids as Additives for Lubricating Oils. *Tribol. Int.* **2006**, *39*, 560−564.

(4) Aschmann, S. M.; Atkinson, R. Rate Constants for the Gas-Phase Reactions of Selected Dibasic Esters with the OH Radical. *Int. J. Chem. Kinet.* **1998**, *30*, 471−474.

(5) Cavalli, F.; Barnes, I.; Becker, K. H. FT-IR Kinetic and Product Study of the OH Radical and Cl-Atom-Initiated Oxidation of Dibasic Esters. *Int. J. Chem. Kinet.* **2001**, *33*, 431−439.

(6) Tuazon, E. C.; Aschmann, S. M.; Atkinson, R. Products of the Gas-Phase Reaction of the OH Radical with the Dibasic Ester $CH_3OC(O)CH_2CH_2CH_2C(O)OCH_3$. *Environ. Sci. Technol.* **1999**, *33*, 2885−2890.

(7) Ashnagar, A.; Gharib naseri, N.; Sheeri, B. Novel Synthesis of Barbiturates. *Chin. J. Chem.* **2007**, *25*, 382−384.

(8) Mahmudov, K. T.; Kopylovich, M. N.; Maharramov, A. M.; Kurbanova, M. M.; Gurbanov, A. V.; Pombeiro, A. J. L. Barbituric Acids as a Useful Tool for the Construction of Coordination and Supramolecular Compounds. *Coord. Chem. Rev.* **2014**, *265*, 1−37.

(9) Schaefer, B. *Natural Products in the Chemical Industry*; Springer, 2014.

(10) Selvakumar, N.; Yadi Reddy, B.; Sunil Kumar, G.; Iqbal, J. Dimethyl Malonate as a One-Carbon Source: A Novel Method of Introducing Carbon Substituents onto Aromatic Nitro Compounds. *Tetrahedron Lett.* **2001**, *42*, 8395−8398.

(11) Henao, D.; Pelaez, W.; Argüello, G. A.; Malanca, F. E. Photooxidation of Di-Tert-Butyl Malonate in the Presence and Absence of Nitrogen Dioxide. *J. Phys. Chem. A* **2016**, *120*, 8267−8272.

(12) Atkinson, R. Kinetics and Mechanisms of the Gas-Phase Reactions of the Hydroxyl Radical with Organic Compounds under Atmospheric Conditions. *Chem. Rev.* **1986**, *86*, 69−201.

(13) Frisch, M. J.; Trucks, G. W.; Schlegel, H. B.; Scuseria, G. E.; Robb, M. A.; Cheeseman, J. R.; Scalmani, G.; Barone, V.; Petersson, G. A.; Nakatsuji, H.; et al. *Gaussian 09*, revision A.02; Gaussian, Inc.: Wallingford, CT, 2009.

(14) Kohn, W.; Becke, A. D.; Parr, R. G. Density Functional Theory of Electronic Structure. *J. Phys. Chem.* **1996**, *100*, 12974−12980.

(15) Notario, A.; Mellouki, A.; Le Bras, G. Rate Constants for the Gas-Phase Reactions of Chlorine Atoms with a Series of Ketones. *Int. J. Chem. Kinet.* **2000**, *32*, 62−66.

(16) Albaladejo, J.; Notario, A.; Cuevas, C. A.; Jiménez, E.; Cabañas, B.; Martínez, E. Gas-Phase Chemistry of Atmospheric Cl Atoms: A PLP-RF Kinetic Study with a Series of Ketones. *Atmos. Environ.* **2003**, *37*, 455−463.

(17) Sellevag, S. R.; Nielsen, C. J. Kinetic Study of the Reactions CH_2ClCH_2Cl + OH, $CH_3C(O)CH_3$ + Cl and $HC(O)OCH_2CH_3$ + Cl by the Relative Rate Method. *Asian Chem. Lett.* **2003**, *7*, 15−20.

(18) Carr, S.; Shallcross, D. E.; Canosa-Mas, C. E.; Wenger, J. C.; Sidebottom, H. W.; Treacy, J. J.; Wayne, R. P. A Kinetic and Mechanistic Study of the Gas-Phase Reactions of OH Radicals and Cl Atoms with Some Halogenated Acetones and Their Atmospheric Implications. *Phys. Chem. Chem. Phys.* **2003**, *5*, 3874−3883.

(19) Romanias, M. N.; Stefanopoulos, V. G.; Papanastasiou, D. K.; Papadimitriou, V. C.; Papagiannakopoulos, P. Temperature-Dependent Rate Coefficients and Mechanism for the Gas-Phase Reaction of Chlorine Atoms with Acetone. *Int. J. Chem. Kinet.* **2010**, *42*, 724−734.

(20) Orlando, J. J.; Tyndall, G. S.; Wallington, T. J. The Atmospheric Chemistry of Alkoxy Radicals. *Chem. Rev.* **2003**, *103*, 4657−4689.

(21) Martínez, E.; Aranda, A.; Díaz-De-Mera, Y.; Rodríguez, A.; Rodríguez, D.; Notario, A. Mechanistic and Kinetic Study of the Gas-Phase Reaction of Atomic Chlorine with Cyclohexanone Using an Absolute and a Relative Technique; Influence of Temperature. *J. Atmos. Chem.* **2004**, *48*, 283−299.

(22) Takahashi, K.; Iwasaki, E.; Matsumi, Y.; Wallington, T. J. Pulsed Laser Photolysis Vacuum UV Laser-Induced Fluorescence Kinetic Study of the Gas-Phase Reactions of Cl Atoms with C-3-C-6 Ketones. *J. Phys. Chem. A* **2007**, *111*, 1271−1276.

(23) Zhao, Z.; Huskey, D. T.; Nicovich, J. M.; Wine, P. H. Temperature-Dependent Kinetics Study of the Gas-Phase Reactions of Atomic Chlorine with Acetone, 2-Butanone, and 3-Pentanone. *Int. J. Chem. Kinet.* **2008**, *40*, 259−267.

(24) Atkinson, R.; Baulch, D. L.; Cox, R. A.; Crowley, J. N.; Hampson, R. F.; Hynes, R. G.; Jenkin, M. E.; Rossi, M. J.; Troe, J. IUPAC Task Group on Atmospheric Chemical Kinetic Data Evaluation. *Atmos. Chem. Phys.* **2004**, *4*, 1461−1738.

(25) Notario, A.; LeBras, G.; Mellouki, A. Absolute Rate Constants for the Reactions of Cl Atoms with a Seies of Esters. *J. Phys. Chem. A* **1998**, *102*, 3112−3117.

(26) Good, D. A.; Hansen, J.; Kamoboures, M.; Santiono, R.; Francisco, J. S. An Experimental and Computational Study of the Kinetics and Mechanism of the Reaction of Methyl Formate with Cl Atoms. *J. Phys. Chem. A* **2000**, *104*, 1505−1511.

(27) Atkinson, R. A Structure-Activity Relationship for the Estimation of Rate Constants for the Gas-Phase Reactions of OH Radicals with Organic Compounds. *Int. J. Chem. Kinet.* **1987**, *19*, 799−828.

(28) Kwok, E. S. C.; Atkinson, R. Estimation of Hydroxyl Radical Reaction Rate Constants for Gas-Phase Organic Compounds Using a Structure-Reactivity Relationship: An Update. *Atmos. Environ.* **1995**, *29*, 1685−1695.

(29) Yoshida, H.; Takeda, K.; Okamura, J.; Ehara, A.; Matsuura, H. A New Approach to Vibrational Analysis of Large Molecules by Density Functional Theory: Wavenumber-Linear Scaling Method. *J. Phys. Chem. A* **2002**, *106*, 3580−3586.

(30) Ferenac, M. A.; Davis, A. J.; Holloway, A. S.; Dibble, T. S. Isomerization and Decomposition Reactions of Primary Alkoxy Radicals Derived from Oxygenated Solvents. *J. Phys. Chem. A* **2003**, *107*, 63−72.

(31) Christensen, L. K.; Ball, J. C.; Wallington, T. J. Atmospheric Oxidation Mechanism of Methyl Acetate. *J. Phys. Chem. A* **2000**, *104*, 345−351.

(32) Atkinson, R.; Baulch, D. L.; Cox, R. A.; Crowley, J. N.; Hampson, R. F.; Hynes, R. G.; Jenkin, M. E.; Rossi, M. J.; Troe, J. Evaluated Kinetic and Photochemical Data for Atmospheric Chemistry: Volume II − Gas Phase Reactions of Organic Species The IUPAC Subcommittee on Gas Kinetic Data Evaluation for Atmospheric Chemistry. *Atmos. Chem. Phys.* **2006**, *6*, 3625−4055.

DOI: 10.1021/acs.jpca.7b06595
J. Phys. Chem. A XXXX, XXX, XXX−XXX